

Sample-efficient Real-time Planning with Curiosity Cross-Entropy Method and Contrastive Learning

Mostafa Kotb^{1,2,*}, Cornelius Weber¹, and Stefan Wermter¹

Abstract—Model-based reinforcement learning (MBRL) with real-time planning has shown great potential in locomotion and manipulation control tasks. However, the existing planning methods, such as the Cross-Entropy Method (CEM), do not scale well to complex high-dimensional environments. One of the key reasons for underperformance is the lack of exploration, as these planning methods only aim to maximize the cumulative extrinsic reward over the planning horizon. Furthermore, planning inside the compact latent space in the absence of observations makes it challenging to use curiosity-based intrinsic motivation. We propose Curiosity CEM (CCEM), an improved version of the CEM algorithm for encouraging exploration via curiosity. Our proposed method maximizes the sum of state-action Q values over the planning horizon, in which these Q values estimate the future extrinsic and intrinsic reward, hence encouraging reaching novel observations. In addition, our model uses contrastive representation learning to efficiently learn latent representations. Experiments on image-based continuous control tasks from the DeepMind Control suite show that CCEM is by a large margin more sample-efficient than previous MBRL algorithms and compares favorably with the best model-free RL methods.

I. INTRODUCTION

Model-based RL (MBRL) improves sample efficiency by learning a dynamics model in latent space, then either utilizes the learned model directly for real-time (online) planning [1][2] or optimizes a policy inside imagined trajectories (i.e., background planning) [3]. MBRL has shown outstanding successes in complex discrete environments, such as defeating human world champions in chess [4] and Go [5]. However, in continuous control tasks, planning methods such as the Cross-Entropy Method (CEM) [6] do not scale well with the increasing complexity in environments. The way of planning by randomly generating action sequences and then executing the first action in the sequence with the highest expected reward, is inefficient in complex high-dimensional environments [7][8].

Furthermore, CEM lacks exploration as it only aims to maximize the extrinsic reward of the sampled action sequences, therefore it might fail in sparse reward settings and hard-to-explore environments with high-dimensional state and action spaces. Consequently, no MBRL algorithm has yet achieved the asymptotic performance as the best model-free RL (MFRL) algorithm on image-based continuous control tasks [9].

¹The authors are with the Knowledge Technology Group, Department of Informatics, Universität Hamburg, 22527 Hamburg, Germany. E-mail: {mostafa.kotb, cornelius.weber, stefan.wermter}@uni-hamburg.de.

²Mathematics Department, Faculty of Science, Aswan University, 81528 Aswan, Egypt.

*Corresponding author, Email: mostafa.kotb@uni-hamburg.de.

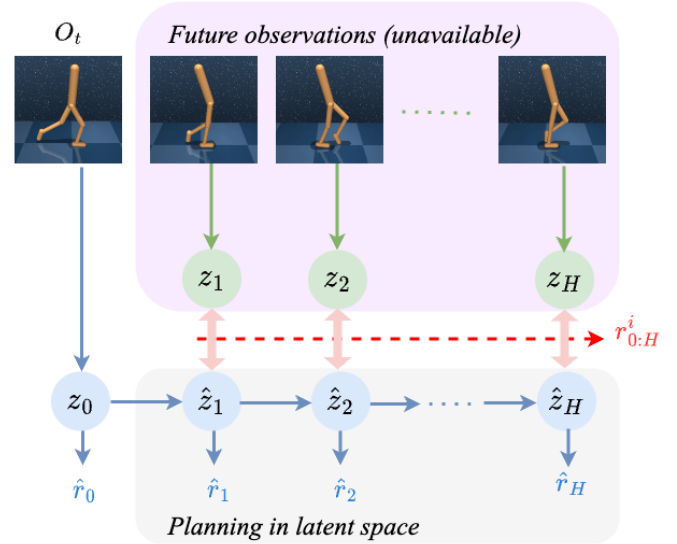


Fig. 1: **The difficulty of using intrinsic reward during planning:** At every time step, the observation o_t is encoded into latent state z_0 . Then, the planner, with the help of the learned latent model, samples a trajectory of the predicted latent states $\hat{z}_{1:H}$ and extrinsic rewards $\hat{r}_{0:H}$. The future observations are not available during planning, therefore the intrinsic rewards $r^i_{0:H}$ cannot be estimated as the prediction error between the actual latent states $z_{1:H}$ and the predicted latent states $\hat{z}_{1:H}$, (as shown by the dashed red arrow).

An effective approach to improve exploration is to use curiosity-based intrinsic reward as the prediction error of the next latent state (i.e., prediction-based exploration) [10][11][12], which encourages reaching novel states. Curiosity-based intrinsic motivation has been used extensively with MFRL [10][12][13][14], but is still rarely used with MBRL [15]. Unfortunately, it is technically challenging to use such intrinsic reward with MBRL planning methods, especially real-time planning (see Fig. 1), as the ground truth future observations are unavailable during planning, and hence the prediction error cannot be estimated.

A solution proposed in Plan2Explore [15] is to compute the intrinsic reward as the disagreement in the predicted next latent state from an ensemble of forward dynamics models (FDM). However, training an ensemble of FDM with latent dynamics model is computationally intensive and requires careful balancing of the heterogeneity of the population.

In this paper, to alleviate the aforementioned challenges with real-time planning, we propose *Curiosity CEM*

(CCEM), an improved version of CEM for encouraging exploration via curiosity. We take a different route from Plan2Explore, instead of estimating the intrinsic reward *online* during planning using an ensemble of FDM, our proposed method estimates the intrinsic reward *offline* during training. To this end, we train a state-value Q function to estimate future extrinsic and intrinsic reward. During planning, the proposed Curiosity CEM maximizes the sum of these Q values over the planning horizon, hence encouraging reaching novel states. An *Intrinsic Curiosity Module (ICM)* [10] is used to estimate the curiosity-based intrinsic reward. To further improve sample efficiency, we use contrastive representation learning by maximizing the temporal mutual information between embeddings of consecutive time steps [16][17][18]. We choose TD-MPC [2] as the model-based RL to evaluate our proposed CCEM and we name it *TD-MPC with CCEM*.

We evaluate the sample efficiency of our proposed method on six image-based continuous control tasks from the DeepMind Control Suite [19]. Our proposed method outperforms state-of-the-art MFRL methods at the 100k environment step, particularly outperforming previous MBRL algorithms by a large margin, showing its superiority as a real-time planning method. The contributions of our work are as follows:

- We propose CCEM, a real-time planning method for encouraging exploration via curiosity.
- We demonstrate the robustness of CCEM as a real-time planner by comparing it against two variants of CEM.
- We show that TD-MPC with CCEM is more sample efficient than previous MBRL methods.

To the best of our knowledge, this is the first time a curiosity-based exploration technique is used to improve the performance of a real-time planning MBRL algorithm.

II. RELATED WORK

A. Curiosity-based Exploration

RL agents are trained by maximizing the cumulative extrinsic reward that is often designed as a dense well-shaped reward [20] to facilitate the completion of the task. However, reward shaping requires domain knowledge and human effort, and thus sparse reward tasks are more common in practice at the cost of a slow learning process [21]. Curiosity-based exploration has been proposed to help agents explore in sparse reward settings and in complex high-dimensional environments. There have been many techniques introduced, such as *visit-counts* [22][23][24] which discourages revisiting same states, and *prediction-based* [10][11][12] which encourages reaching novel states by estimating the intrinsic reward as the prediction error of next state.

Prediction-based exploration has shown to be effective and has been used extensively with model-free agents [13][14][10][12] but has been rarely used with model-based agents [15]. In model-based RL, online planning in the latent space in the absence of the ground truth observations makes it challenging to estimate the intrinsic reward as the prediction error. To overcome this challenge, we propose to

compute the intrinsic reward offline during training, as the ground truth observations are available, then train a Q value function to estimate future extrinsic and intrinsic reward. During planning, we maximize the sum of Q values over the planning horizon.

B. Contrastive Representation Learning

Recently, contrastive learning (CL) [25] has proven effective in learning latent representations and led to improve the sample efficiency of vision-based RL agents. CL learns latent representations in an unsupervised fashion by minimizing the distance in the latent space between two similar images (i.e., positive pairs), and at the same time maximizing the distance between two dissimilar images (i.e., negative pairs).

CURL [26] proposed a contrastive loss between two different data-augmentation of the same observation, while CPC [27] and ST-DIM [16] proposed different variations of temporal contrastive loss between two augmented observations separated by small time steps. To decouple representation learning from policy learning, a new unsupervised learning task called Augmented Temporal Contrast (ATC) was introduced to train the encoder exclusively using a temporal contrastive loss [28]. The result showed that training the representations in an unsupervised way (i.e. not relying on the environment’s reward) is very helpful for multitasking and sparse reward environment. In addition, several contrastive approaches extend MFRL with a predictive model to help learning temporally consistent representations [18][29][30].

Reconstruction-free model-based RL [31] [32] [33] [34] learns a world model in a contrastive way without reconstructing the observations. These models succeeded in learning task-related representations in complex observations where task-irrelevant information are presented as distractions. In our work, we use a temporal contrastive loss between the joint representations of an observation and action and the representation of the next observation [18].

III. BACKGROUND

A. Reinforcement learning from images with intrinsic reward

We formulate the problem of imaged-based continuous control as an infinite-horizon Markov Decision Process (MDP). An MDP characterized by a tuple $(\mathcal{O}, \mathcal{A}, \mathcal{R}, \mathcal{P}, \gamma)$, where \mathcal{O} is the high-dimensional observation space (RGB image pixels), \mathcal{A} is the continuous action space, $\mathcal{P} : \mathcal{O} \times \mathcal{A} \times \mathcal{O} \mapsto \mathbb{R}_+$ is the transition function, $\mathcal{R} : \mathcal{O} \times \mathcal{A} \mapsto \mathbb{R}$ is a reward function (also known as extrinsic reward r_t^e), and $\gamma \in [0, 1]$ is a discount factor. The goal of RL is to learn a parameterized mapping policy $\Pi_\theta : \mathcal{O} \mapsto \mathcal{A}$, that maximizes the expected cumulative reward $\mathbb{E}_{a_t \sim \Pi_\theta} [\sum_{t=0}^{\infty} \gamma^t r_t^e]$.

To encourage exploration and avoid the policy from getting stuck in a local minimal, exploration bonuses are given as *intrinsic reward* r_t^i . Thus, during training, to encourage reaching novel states, the policy has to maximize the new expected cumulative reward $\mathbb{E}_{a_t \sim \Pi_\theta} [\sum_{t=0}^{\infty} \gamma^t (r_t^e + r_t^i)]$.

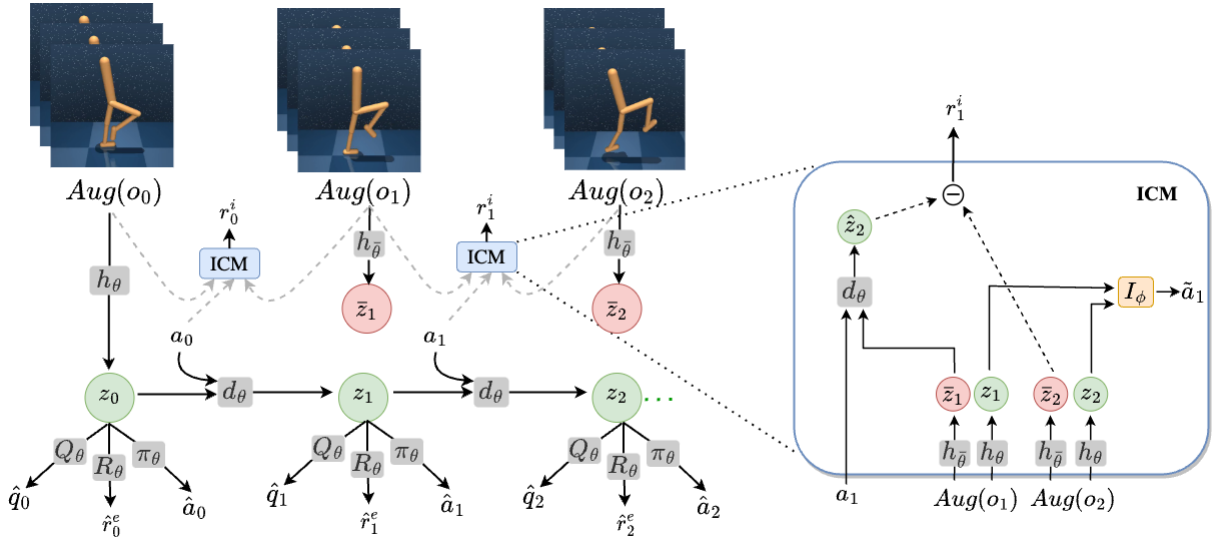


Fig. 2: **Training:** A trajectory of length k is sampled from the replay buffer. The initial observation o_0 is augmented and encoded using encoder h_θ into latent state z_0 , and subsequent observations are augmented and encoded using the target encoder $h_{\bar{\theta}}$. TOLD [2] recurrently predicts latent states z_1, z_2, \dots, z_k , and a Q -value \hat{q}_t , an extrinsic reward \hat{r}_t^e , and an action \hat{a}_t for each latent state z_t . The intrinsic reward r_t^i is computed using ICM [10]. The inverse model I_ϕ takes latent states (z_1, z_2) and predicts action \tilde{a}_1 , and the latent dynamics model d_θ from TOLD takes target latent state \bar{z}_1 extracted by $h_{\bar{\theta}}$ and action a_1 and predicts \hat{z}_2 . The intrinsic reward r_1^i is computed as the prediction error between \hat{z}_2 and \bar{z}_2 .

B. Cross-Entropy Method

Cross-Entropy Method (CEM) [6] is a derivative-free optimization technique that has been used with MBRL as an efficient online planner [1][7][9]. CEM starts by sampling action sequences of length H , where H is the planning horizon, from a time-dependent diagonal Gaussian distribution initialized by zero mean and unit variance $(\mu_{0:H}, \sigma_{0:H})$. Then, the sampled sequences are evaluated based on a *scoring function* and the top k candidates are selected. The distribution μ and σ are fitted to the top k candidates and after several iterations of this procedure, the planner returns the mean for the current time step, μ_t as the best action to be executed. To plan for the next time step, the Gaussian distribution is initialized again to zero mean and unit variance to avoid local optima.

There are three variants of CEM based on three different scoring functions proposed in the literature as follows:

Sum of rewards [9]: Discounted sum of rewards $\sum_{t=0}^H \gamma^t r(o_t, a_t)$, which defines the original CEM.

Sum of rewards + terminal value [35]: Discounted sum of rewards summed with the estimated value of the terminal state $\sum_{t=0}^{H-1} \gamma^t r(o_t, a_t) + \gamma^H Q(o_H, a_H)$, which defines *CEM with terminal value function*.

Sum of values [36]: Discounted sum of state-action values $\sum_{t=0}^H \gamma^t Q(o_t, a_t)$, which defines *CEM with value summation*.

In this paper, we propose *Curiosity CEM*, a fourth variant of CEM for encouraging exploration. The scoring function is the same as sum of values [36], except that the Q values are trained to estimate extrinsic and intrinsic reward.

IV. TD-MPC WITH CURIOSITY CEM

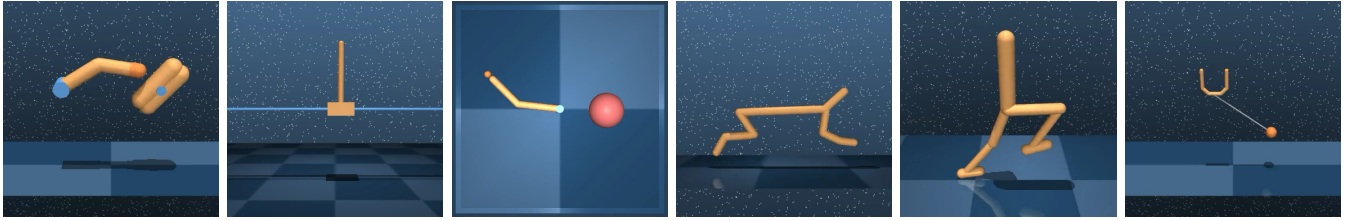
We choose Temporal Difference Model Predictive Control (TD-MPC) [2] as the MBRL to test and evaluate our proposed Curiosity CEM (CCEM) method. The original TD-MPC uses *CEM with terminal value function* as the planning method. In this section, we explain in detail the *training* and *inference* procedures of TD-MPC with CCEM. See Algorithm 1 for training pseudo code.

A. Training

TD-MPC uses a Task-Oriented Latent Dynamics (TOLD) model which is jointly trained together with a terminal Q value function using temporal difference learning. TOLD consists of five model components (shown as gray shaded squares in Fig.2), as follows:

- 1) **Encoder:** $z_t = h_\theta(o_t)$, encodes a given observation o_t into a latent representation z_t .
- 2) **Latent dynamics:** $z_{t+1} = d_\theta(z_t, a_t)$, predicts the next latent representation z_{t+1} given z_t and action a_t .
- 3) **Reward:** $\hat{r}_t^e = R_\theta(z_t, a_t)$, predicts extrinsic reward \hat{r}_t^e given z_t and a_t .
- 4) **Value:** $\hat{q}_t = Q_\theta(z_t, a_t)$, predicts state-action value \hat{q}_t given z_t and a_t .
- 5) **Policy:** $\hat{a}_t \sim \pi_\theta(z_t)$, predicts an action \hat{a}_t that approximately maximizes the Q -function.

Our proposed CCEM computes the curiosity-based intrinsic reward r_t^i *offline* during training using *Intrinsic Curiosity Module (ICM)* [10]. As shown in Fig.2, ICM consists of an inverse dynamics model I_ϕ that takes the latent representations of two consecutive observations and predicts the action taken to move from o_t to o_{t+1} , $\tilde{a}_t = I_\phi(h_\theta(o_t), h_\theta(o_{t+1}))$.



(a) Finger Spin (b) Cartpole Swingup (c) Reacher Easy (d) Cheetah Run (e) Walker Walk (f) Ball-in-cup Catch

Fig. 3: Image-based continuous control tasks from the DeepMind Control Suite (DMC). These benchmark tasks introduce a diverse set of challenges: sparse reward (e.g., Ball-in-cup, Reacher), complex dynamics (e.g., Walker, Finger, Cheetah), hard exploration (e.g., Walker, Cheetah), and partial observability (e.g., Cartpole as the cart can move out of sight).

The inverse model is trained by minimizing the following prediction error:

$$\mathcal{L}_t^{\mathcal{I}}(\phi, \theta_h) = \|\tilde{a}_t - a_t\|_2^2. \quad (1)$$

In addition to the inverse dynamics model, a forward dynamics model is required to compute the intrinsic reward as the error in predicting the next latent state. Instead of defining a separate FDM, we make use of the latent dynamics d_θ in the TOLD model. The next latent state is predicted as $\hat{z}_{t+1} = d_\theta(\bar{z}_t, a_t)$,

where $\bar{z}_t = h_{\bar{\theta}}(o_t)$ is extracted using the target encoder $h_{\bar{\theta}}$, whose parameters are an exponential moving average (EMA) of the online encoder h_θ [37][38].

We follow [30] in normalizing and decaying the intrinsic reward during training to converge to the optimal solutions. The intrinsic reward is computed as follows:

$$r_t^i = C e^{-\alpha E_t} \cdot \|\hat{z}_{t+1} - \bar{z}_{t+1}\|_2^2 \cdot \left(\frac{r_e^{max}}{r_i^{max}} \right), \quad (2)$$

where C is the intrinsic weight, α is the decay weight, E_t is environment step, r_e^{max} and r_i^{max} are the maximum extrinsic and intrinsic reward, respectively.

After computing the intrinsic reward, the state-action value function Q_θ is trained with temporal difference learning to estimate future extrinsic and intrinsic reward by minimizing the following objective:

$$\mathcal{L}_t^{\mathcal{Q}} = \|Q_\theta(z_t, a_t) - (r_t^e + r_t^i + \gamma Q_{\bar{\theta}}(z_{t+1}, \pi_\theta(z_{t+1})))\|_2^2, \quad (3)$$

where $Q_{\bar{\theta}}$ is a target Q -function which is an EMA of Q_θ , γ is a discount factor, and the policy π_θ is trained to maximize Q_θ by minimizing the following objective:

$$\mathcal{L}_t^\pi = -Q_\theta(z_t, \pi_\theta(z_t)), \quad (4)$$

where the policy objective is only optimized with respect to the policy parameters θ_π . The reward model R_θ is trained by minimizing the prediction error between the predicted and the ground truth extrinsic reward:

$$\mathcal{L}_t^{\mathcal{R}} = \|R_\theta(z_t, a_t) - r_t^e\|_2^2. \quad (5)$$

In order to learn temporally predictive and consistent latent representations that are invariant to data augmentation, the subsequent observations are augmented and encoded using

the target encoder $h_{\bar{\theta}}$, and a latent consistency loss is used, which is defined as follows:

$$\mathcal{L}_t^{\mathcal{C}} = \|d_\theta(z_t, a_t) - h_{\bar{\theta}}(o_{t+1})\|_2^2. \quad (6)$$

Finally, the proposed TD-MPC with CCEM is trained by sampling a trajectory $\Gamma = (o_t, a_t, r_t^e, o_{t+1})_{t:t+K}$ from the replay buffer \mathcal{B} . Then, the TOLD model is updated by minimizing the following temporally weighted objective:

$$\mathcal{L}^{TOLD}(\theta) = \sum_{i=t}^{t+K} \lambda^{i-t} (c_1 \cdot \mathcal{L}_i^{\mathcal{Q}} + c_2 \cdot \mathcal{L}_i^{\mathcal{R}} + c_3 \cdot \mathcal{L}_i^{\mathcal{C}} + \mathcal{L}_i^\pi), \quad (7)$$

where λ is a constant that assigns higher weight to near-term predictions, c_1, c_2, c_3 are loss coefficients, and $\mathcal{L}_i^{\mathcal{Q}}, \mathcal{L}_i^{\mathcal{R}}, \mathcal{L}_i^{\mathcal{C}}, \mathcal{L}_i^\pi$ are the single-step objectives from Eq. 3, 5, 6, 4, respectively. The inverse dynamics model is updated by minimizing the following objective:

$$\mathcal{L}^{Inv}(\phi, \theta_h) = \sum_{i=t}^{t+K} \mathcal{L}_i^{\mathcal{I}}, \quad (8)$$

where $\mathcal{L}_i^{\mathcal{I}}$ is the single-step objective from Eq. 1.

Contrastive Learning: To efficiently learn representations, we use contrastive learning in the form of maximizing the temporal mutual information between the joint representations of the current observation and action and the representation of the next observation [18]. We introduce an action encoder g_ψ that maps an action a_t into a latent feature vector u_t . From the sampled trajectory $\Gamma_{t:t+k}$, we only use (o_t, a_t, o_{t+1}) . The observations o_t and o_{t+1} are augmented and encoded using the online encoder h_θ and the target encoder $h_{\bar{\theta}}$, respectively

$$z_t = h_\theta(o_t), \quad \bar{z}_{t+1} = h_{\bar{\theta}}(o_{t+1}). \quad (9)$$

The *query* is the joint representations of current observation o_t and action a_t referred to as $c(z_t, u_t)$, where $c(\cdot, \cdot)$ is a concatenating operation, while the representation of next observation o_{t+1} referred to as \bar{z}_{t+1} is the *key*.

We apply InfoNCE loss [27] using similarity measure computed as a bilinear product $(c(z_t, u_t)^T W \bar{z}_{t+1})$, where W is a learnable *contrastive transformation matrix*. The

Algorithm 1: TD-MPC with CCEM (Training)

Require: network parameters $(\theta, \bar{\theta}, \phi, \psi)$, replay buffer \mathcal{B} , learning rates (η_m, η_i, η_c) , EMA coefficient ζ , and ICM [10]

for each training step do

$\mathcal{B} \leftarrow \mathcal{B} \cup (o_t, a_t, r_t^e, o_{t+1})_{t=0:T-1}$; \triangleright Collect ep.

for num updates per episode do

$(o_t, a_t, r_t^e, o_{t+1})_{t:t+k} \sim \mathcal{B}$; \triangleright Sample traj.

$z_t = h_\theta(o_t)$; \triangleright Encode first observation.

for $j = t$ to $t+k$ do

$\hat{r}_j^e = R_\theta(z_j, a_j)$; \triangleright ext. reward

$\hat{q}_j = Q_\theta(z_j, a_j)$; \triangleright Q value

$\hat{a}_j \sim \pi_\theta(z_j)$; \triangleright policy action

$z_{j+1} = d_\theta(z_j, a_j)$; \triangleright next state

$r_j^i = ICM(o_j, a_j, o_{j+1})$; \triangleright int. reward

end

Update TOLD model:
 $\theta \leftarrow \theta - \eta_m \nabla_\theta \mathcal{L}^{TOLD}(\theta)$;

Update online encoder and inverse dynamics:
 $\{\phi, \theta_h\} \leftarrow \{\phi, \theta_h\} - \eta_i \nabla_{\{\phi, \theta_h\}} \mathcal{L}^{Inv}(\phi, \theta_h)$;

Update online encoder and action encoder:
 $\{\psi, \theta_h\} \leftarrow \{\psi, \theta_h\} - \eta_c \nabla_{\{\psi, \theta_h\}} \mathcal{L}^T(\psi, \theta_h)$;

Update target encoder and target Q-function:
 $\bar{\theta} \leftarrow (1 - \zeta)\bar{\theta} + \zeta\theta$

end

end

temporal contrastive loss is computed as follows:

$$\mathcal{L}^T(\theta_h, \psi) = -\log \left[\frac{\exp(c(z_t, u_t)^T W \bar{z}_{t+1})}{\sum_{\bar{z}_{t+1}^j \in \chi} \exp(c(z_t, u_t)^T W \bar{z}_{t+1}^j)} \right], \quad (10)$$

where χ is the set of all keys (*positive and negative keys*).

B. Inference

During planning, we follow TD-MPC [2] except that, CCEM computes a *discounted sum of Q values* over the planning horizon as the scoring function to evaluate the sampled action sequences as follows:

$$\mathcal{F}_\Gamma = \mathbb{E}_\Gamma \left[\sum_{t=0}^H \gamma^t Q_\theta(z_t, a_t) \right], \quad (11)$$

where Γ is a sampled action sequence, H is the planning horizon, and γ is a discount factor. Since Q_θ is trained by Eq. 3 to estimate extrinsic and intrinsic reward, CCEM encourages exploring novel states.

V. EXPERIMENT

A. Experiment Setup

The proposed method is evaluated on six image-based continuous control tasks from the DeepMind Control Suite (DMC) [19]. These tasks, shown in Fig.3, are considered a standard benchmark for evaluating image-based RL algorithms in terms of sample efficiency [26][39].

Baselines: We compare against previous MBRL algorithms *TD-MPC*[2], *PlaNet*[1], and *Dreamer*[3]. TD-MPC and PlaNet use real-time planning with 2 different variants of CEM, and Dreamer performs background planning. We also compare our method against state-of-the-art visual-based MFRL algorithms, such as *CCFDM*[30], *CoDy*[18], *DrQ*[39], and *CURL*[26]. All algorithms including ours use raw images as inputs, except for *SAC-State* [40], which is presented as an upper bound performance as it receives the direct state input from the simulator.

B. Implementations

We use the implementation of TD-MPC¹ as the baseline to extend to *TD-MPC with CCEM*. We extend the base architecture of TD-MPC by adding an inverse dynamics model I_ϕ and an action encoder g_ψ . The inverse dynamics model is implemented using 2-layer MLP with dimension 512 and the action encoder is implemented using a 1-layer MLP with dimension 512 and all layers use ELU activations. The action encoder applies layer normalization [41] at the output layer. As observations, 3 stacked frames of (84×84) RGB images are used and we perform ± 4 pixel shift augmentation [39]. The target EMA coefficient ζ is set to 0.01. The target Q-function $Q_{\bar{\theta}}$ update frequency is 2, while the target encoder $h_{\bar{\theta}}$ update frequency is 1. The weight constant λ is set to 0.5 and the loss coefficients c_1, c_2, c_3 are set to 0.1, 0.5, and 2, respectively. For the temporal contrastive loss, we find that a coefficient of 2 gives the best performance. We use Adam optimizer with learning rates $(3 \times 10^{-4}, 3 \times 10^{-4}, 1 \times 10^{-5})$ for (η_m, η_i, η_c) , respectively, and batch size of 256. The intrinsic decaying weight α is set to 1×10^{-5} . These mentioned settings are the same for all control tasks. The only task-dependent hyperparameters are the intrinsic weight C and the action repeat (see Table I).

TABLE I: Per-task hyperparameters

Task	Intrinsic weight(C)	Action Repeat
Finger Spin	0.4	2
Cartpole Swingup	0.2	8
Reacher Easy	0.3	4
Cheetah Run	0.2	4
Walker Walk	0.2	2
Ball-in-cup Catch	0.3	4

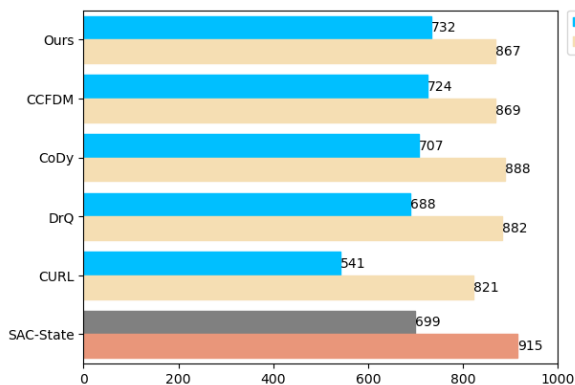
C. Results and Discussion

We run experiments for our proposed method and TD-MPC [2]. For the baselines, we use the results provided in the corresponding papers, except for CURL and Dreamer, where we use the results provided in [18], and for PlaNet, where we use the results provided in [30]. For fair comparison, we follow the settings proposed in [26]. Every agent is evaluated after every 10k environment steps, averaging over 10 episodes, then the averaged return is logged. The sample efficiency is measured by the performance at 100k environment steps, which is the relevant measure for learning

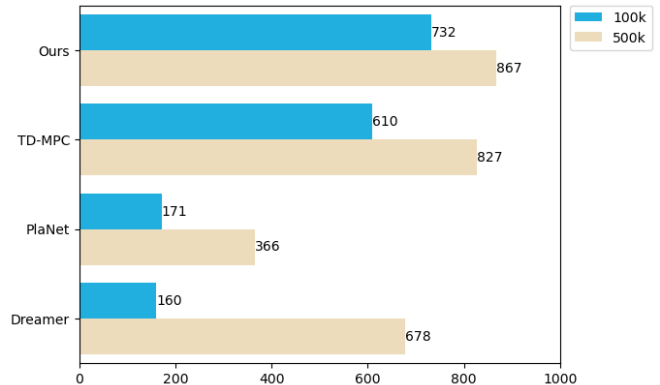
¹<https://github.com/nicklashansen/tdmpc>

TABLE II: Average return (mean and standard deviations) across 5 random seeds achieved by our method and baselines on DMC [19] evaluated at 100k and 500k environment step. Our method outperforms MBRL baselines by a large margin and achieves the highest average return on 4 out of 6 tasks at 100k environment step. SAC-State is an upper bound performance.

100k step scores	Model-free					Model-based			Ours
	SAC-State [40]	CCFDM [30]	CoDy [18]	DrQ [39]	CURL [18]	PlaNet [30]	Dreamer [18]	TD-MPC [2]	
Finger Spin	672 ± 76	880 ± 142	887 ± 39	901 ± 104	750 ± 37	95 ± 164	33 ± 19	899 ± 146	951 ± 40
Cartpole Swingup	812 ± 45	785 ± 87	784 ± 18	759 ± 92	547 ± 73	303 ± 71	235 ± 73	747 ± 78	753 ± 60
Reacher Easy	919 ± 123	811 ± 220	624 ± 42	601 ± 213	460 ± 65	140 ± 256	148 ± 53	413 ± 62	632 ± 101
Cheetah Run	228 ± 95	274 ± 98	323 ± 29	344 ± 67	266 ± 27	165 ± 123	159 ± 60	274 ± 69	362 ± 37
Walker Walk	604 ± 317	634 ± 132	673 ± 94	612 ± 164	482 ± 28	125 ± 57	216 ± 56	653 ± 99	731 ± 49
Ball-in-cup Catch	957 ± 26	962 ± 28	948 ± 6	913 ± 53	741 ± 102	198 ± 442	172 ± 96	675 ± 221	964 ± 3
500k step scores									
Finger Spin	927 ± 43	906 ± 152	937 ± 41	938 ± 103	854 ± 48	418 ± 382	320 ± 35	985 ± 4	980 ± 9
Cartpole Swingup	870 ± 7	875 ± 38	869 ± 4	868 ± 10	837 ± 15	464 ± 50	711 ± 94	860 ± 11	864 ± 6
Reacher Easy	975 ± 5	973 ± 36	957 ± 16	942 ± 71	891 ± 30	351 ± 483	581 ± 160	722 ± 184	907 ± 56
Cheetah Run	772 ± 60	552 ± 130	656 ± 43	660 ± 96	492 ± 22	321 ± 104	571 ± 109	488 ± 74	531 ± 49
Walker Walk	964 ± 8	929 ± 68	943 ± 17	921 ± 46	897 ± 26	293 ± 114	924 ± 35	944 ± 15	946 ± 6
Ball-in-cup Catch	979 ± 6	979 ± 17	970 ± 4	963 ± 9	957 ± 6	352 ± 467	966 ± 8	967 ± 15	975 ± 5



(a) Ours VS. MFRL



(b) Ours VS. MBRL

Fig. 4: Evaluation Score Performance of TD-MPC with CCEM averaged over six tasks relative to (a) model-free RL algorithms, (b) model-based RL algorithms. Our method outperforms all model-free baselines at 100k environment step and nearly reaches SAC-State, the upper bound performance. Our method outperforms all model-based RL baselines, as well.

speed. Also, values at 500k environment steps are given, which are near convergence. For each task, every algorithm is trained with 5 seeds and the result is reported in Table II.

The result shows that TD-MPC with CCEM achieves better sample efficiency at 100k environment steps against all baseline algorithms. TD-MPC with CCEM achieves the highest average return on four out of six tasks at 100k environment steps and close to CCFDM [30] on the other two tasks (i.e., Cartpole-Swingup and Reacher-Easy). Our method demonstrates a stable performance with the lowest standard deviations together with CoDy [18] across all tasks which means that it is less sensitive against different seeds.

According to Fig. 4 that shows the average result over six tasks, our method outperforms all MFRL baselines at 100k steps and nearly matches SAC-State [40] Fig. 4a, the upper bound performance, and outperforms MBRL baselines by a large margin Fig. 4b. TD-MPC with CCEM is the state-of-the-art MBRL algorithm in terms of sample-efficiency which proves the robustness of CCEM as a planning method.

VI. CONCLUSION

This paper proposed the Curiosity Cross-Entropy Method (CCEM), a robust planning method for encouraging exploration via curiosity. CCEM shows that using curiosity-based intrinsic reward with the real-time planning method improves the exploration significantly and leads to better sample efficiency. CCEM can enhance the performance of any MBRL agent as it does not require predefined conditions. CCEM provides state-of-the-art performance in terms of sample efficiency by incorporating it with TD-MPC that uses contrastive representation learning on image-based control tasks. For future research, we plan to evaluate CCEM with other MBRL algorithms and test it in robotic manipulation.

Acknowledgement. The authors thank Philipp Allgeuer for revising the final draft of the paper. The authors gratefully acknowledge support from the German Research Foundation DFG under project CML (TRR 169). Mostafa Kotb is funded by a scholarship from the Ministry of Higher Education of the Arab Republic of Egypt.

REFERENCES

- [1] D. Hafner, T. Lillicrap, I. Fischer, R. Villegas, D. Ha, H. Lee, and J. Davidson, "Learning latent dynamics for planning from pixels," in *International Conference on Machine Learning*. PMLR, 2019, pp. 2555–2565.
- [2] N. Hansen, X. Wang, and H. Su, "Temporal difference learning for model predictive control," in *Proceedings of the 39th International Conference on Machine Learning (ICML)*, 2022.
- [3] D. Hafner, T. Lillicrap, J. Ba, and M. Norouzi, "Dream to control: Learning behaviors by latent imagination," in *International Conference on Learning Representations*, 2020.
- [4] M. Campbell, A. J. Hoane Jr, and F.-h. Hsu, "Deep blue," *Artificial intelligence*, vol. 134, no. 1-2, pp. 57–83, 2002.
- [5] D. Silver, A. Huang, C. J. Maddison, A. Guez, L. Sifre, G. Van Den Driessche, J. Schrittwieser, I. Antonoglou, V. Panneershelvam, M. Lanctot, *et al.*, "Mastering the game of go with deep neural networks and tree search," *nature*, vol. 529, no. 7587, pp. 484–489, 2016.
- [6] R. Rubinfeld, "The cross-entropy method for combinatorial and continuous optimization," *Methodology and Computing in Applied Probability*, vol. 1, pp. 127–190, 1999.
- [7] T. Wang and J. Ba, "Exploring model-based planning with policy networks," *arXiv preprint arXiv:1906.08649*, 2019.
- [8] A. Nagabandi, G. Kahn, R. S. Fearing, and S. Levine, "Neural network dynamics for model-based deep reinforcement learning with model-free fine-tuning," in *2018 IEEE International Conference on Robotics and Automation (ICRA)*. IEEE, 2018, pp. 7559–7566.
- [9] K. Chua, R. Calandra, R. McAllister, and S. Levine, "Deep reinforcement learning in a handful of trials using probabilistic dynamics models," *Advances in Neural Information Processing Systems*, vol. 31, 2018.
- [10] D. Pathak, P. Agrawal, A. A. Efros, and T. Darrell, "Curiosity-driven exploration by self-supervised prediction," in *International Conference on Machine Learning*. PMLR, 2017, pp. 2778–2787.
- [11] P.-Y. Oudeyer, F. Kaplan, and V. V. Hafner, "Intrinsic motivation systems for autonomous mental development," *IEEE Transactions on Evolutionary Computation*, vol. 11, no. 2, pp. 265–286, 2007.
- [12] Y. Burda, H. Edwards, D. Pathak, A. Storkey, T. Darrell, and A. A. Efros, "Large-scale study of curiosity-driven learning," *arXiv preprint arXiv:1808.04355*, 2018.
- [13] R. Houthoofd, X. Chen, Y. Duan, J. Schulman, F. De Turck, and P. Abbeel, "VIME: Variational information maximizing exploration," *Advances in Neural Information Processing Systems*, vol. 29, 2016.
- [14] S. Mohamed and D. Jimenez Rezende, "Variational information maximisation for intrinsically motivated reinforcement learning," *Advances in Neural Information Processing Systems*, vol. 28, 2015.
- [15] R. Sekar, O. Rybkin, K. Daniilidis, P. Abbeel, D. Hafner, and D. Pathak, "Planning to explore via self-supervised world models," in *International Conference on Machine Learning*. PMLR, 2020, pp. 8583–8592.
- [16] A. Anand, E. Racah, S. Ozair, Y. Bengio, M.-A. Côté, and R. D. Hjelm, "Unsupervised state representation learning in Atari," *Advances in Neural Information Processing Systems*, vol. 32, 2019.
- [17] K.-H. Lee, I. Fischer, A. Liu, Y. Guo, H. Lee, J. Canny, and S. Guadarrama, "Predictive information accelerates learning in RL," *Advances in Neural Information Processing Systems*, vol. 33, pp. 11 890–11 901, 2020.
- [18] B. You, O. Arenz, Y. Chen, and J. Peters, "Integrating contrastive learning with dynamic models for reinforcement learning from images," *Neurocomputing*, vol. 476, pp. 102–114, 2022.
- [19] S. Tunyasuvunakool, A. Muldal, Y. Doron, S. Liu, S. Bohez, J. Merel, T. Erez, T. Lillicrap, N. Heess, and Y. Tassa, "dm_control: Software and tasks for continuous control," *Software Impacts*, vol. 6, p. 100022, 2020.
- [20] Y. Hu, W. Wang, H. Jia, Y. Wang, Y. Chen, J. Hao, F. Wu, and C. Fan, "Learning to utilize shaping rewards: A new approach of reward shaping," *Advances in Neural Information Processing Systems*, vol. 33, pp. 15 931–15 941, 2020.
- [21] A. Nair, B. McGrew, M. Andrychowicz, W. Zaremba, and P. Abbeel, "Overcoming exploration in reinforcement learning with demonstrations," *2018 IEEE International Conference on Robotics and Automation*, pp. 6292–6299, 2018.
- [22] M. Bellemare, S. Srinivasan, G. Ostrovski, T. Schaul, D. Saxton, and R. Munos, "Unifying count-based exploration and intrinsic motivation," *Advances in Neural Information Processing Systems*, vol. 29, 2016.
- [23] G. Ostrovski, M. G. Bellemare, A. Oord, and R. Munos, "Count-based exploration with neural density models," in *International Conference on Machine Learning*. PMLR, 2017, pp. 2721–2730.
- [24] M. Lopes, T. Lang, M. Toussaint, and P.-Y. Oudeyer, "Exploration in model-based reinforcement learning by empirically estimating learning progress," *Advances in neural information processing systems*, vol. 25, 2012.
- [25] R. Hadsell, S. Chopra, and Y. LeCun, "Dimensionality reduction by learning an invariant mapping," in *2006 IEEE Computer Society Conference on Computer Vision and Pattern Recognition (CVPR'06)*, vol. 2. IEEE, 2006, pp. 1735–1742.
- [26] M. Laskin, A. Srinivas, and P. Abbeel, "CURL: Contrastive unsupervised representations for reinforcement learning," in *International Conference on Machine Learning*. PMLR, 2020, pp. 5639–5650.
- [27] A. v. d. Oord, Y. Li, and O. Vinyals, "Representation learning with contrastive predictive coding," *arXiv preprint arXiv:1807.03748*, 2018.
- [28] A. Stooke, K. Lee, P. Abbeel, and M. Laskin, "Decoupling representation learning from reinforcement learning," in *International Conference on Machine Learning*. PMLR, 2021, pp. 9870–9879.
- [29] M. Schwarzer, A. Anand, R. Goel, R. D. Hjelm, A. C. Courville, and P. Bachman, "Data-efficient reinforcement learning with self-predictive representations," in *International Conference on Learning Representations*, 2021.
- [30] T. Nguyen, T. M. Luu, T. Vu, and C. D. Yoo, "Sample-efficient reinforcement learning with curiosity contrastive forward dynamics model," in *2021 IEEE/RSJ International Conference on Intelligent Robots and Systems (IROS)*. IEEE, 2021, pp. 3471–3477.
- [31] M. Okada and T. Taniguchi, "Dreaming: Model-based reinforcement learning by latent imagination without reconstruction," in *2021 IEEE International Conference on Robotics and Automation (ICRA)*. IEEE, 2021, pp. 4209–4215.
- [32] X. Ma, S. Chen, D. Hsu, and W. S. Lee, "Contrastive variational reinforcement learning for complex observations," *arXiv preprint arXiv:2008.02430*, 2020.
- [33] T. D. Nguyen, R. Shu, T. Pham, H. Bui, and S. Ermon, "Temporal predictive coding for model-based planning in latent space," in *International Conference on Machine Learning*. PMLR, 2021, pp. 8130–8139.
- [34] F. Deng, I. Jang, and S. Ahn, "Dreamerpro: Reconstruction-free model-based reinforcement learning with prototypical representations," in *International Conference on Machine Learning*. PMLR, 2022, pp. 4956–4975.
- [35] V. Feinberg, A. Wan, I. Stoica, M. I. Jordan, J. E. Gonzalez, and S. Levine, "Model-based value expansion for efficient model-free reinforcement learning," in *Proceedings of the 35th International Conference on Machine Learning (ICML 2018)*, 2018.
- [36] M. Raisi, A. Noohian, L. Mccutcheon, and S. Fallah, "Value Summation: A novel scoring function for MPC-based model-based reinforcement learning," *arXiv preprint arXiv:2209.08169*, 2022.
- [37] A. Tarvainen and H. Valpola, "Mean teachers are better role models: Weight-averaged consistency targets improve semi-supervised deep learning results," *Advances in neural information processing systems*, vol. 30, 2017.
- [38] J.-B. Grill, F. Strub, F. Altché, C. Tallec, P. Richemond, E. Buchatskaya, C. Doersch, B. Avila Pires, Z. Guo, M. Gheshlaghi Azar, *et al.*, "Bootstrap your own latent: a new approach to self-supervised learning," *Advances in Neural Information Processing Systems*, vol. 33, pp. 21 271–21 284, 2020.
- [39] I. Kostrikov, D. Yarats, and R. Fergus, "Image augmentation is all you need: Regularizing deep reinforcement learning from pixels," *arXiv preprint arXiv:2004.13649*, 2020.
- [40] T. Haarnoja, A. Zhou, P. Abbeel, and S. Levine, "Soft actor-critic: Off-policy maximum entropy deep reinforcement learning with a stochastic actor," in *International Conference on Machine Learning*. PMLR, 2018, pp. 1861–1870.
- [41] J. L. Ba, J. R. Kiros, and G. E. Hinton, "Layer normalization," *arXiv preprint arXiv:1607.06450*, 2016.